DETECTION OF MICROCALCIFICATIONS IN MAMMOGRAMS USING 2D PREDICTION FILTERING AND A NEW STATISTICAL MEASURE OF THE RIGHT TAIL WEIGHT

B. Acha*, C. Serrano* and R.M. Rangayyan**

* Dep. de Teoría de la Señal y Comunicaciones, University of Seville, Seville, Spain

** Dept. of Electrical and Computer Engineering, University of Calgary, Calgary, Alberta, Canada

bacha@us.es, cserrano@us.es

Abstract: In this paper, a new method to detect microcalcifications in mammograms is presented. The method is based on a candidate selection procedure which consists of a two-dimensional linear prediction adaptive filtering followed by a statistical parameter calculation developed by the authors and called tail ratio (*TR*). The parameter *TR* characterizes the presence of microcalcifications in a ROI, and is extracted from the local probability distribution within a small region surrounding each candidate. Afterward a group of new and previously published features are used to feed a neural network that classifies the candidates into microcalcification or non-microcalcification. The algorithm has been tested with 38 digitized mammograms obtaining a sensitivity of 0.93 for a positive predictive value of 0.88.

Introduction

The availability and proliferation of digital radiographic images have encouraged research in Computer-aided Diagnosis (CAD). A significant part of such research has concentrated on the detection of breast cancer, in view of the fact that women in Western countries have a higher than 1 in 10 chance of developing breast cancer during their life. In particular, many researchers have focused on the detection of microcalcifications [1,2], which are early signs of breast cancer.

Computer-aided mammography has been studied for more than two decades. During this period the sensitivity of detection has improved, with some recent papers reporting more than 90% sensitivity. Nevertheless, the false-positive rate remains high, especially when detecting individual microcalcifications [3]. Therefore, automated interpretation of microcalcifications remains a challenge due to their small size and variable appearance. Furthermore, when located within or superimposed by dense tissues, especially in young women, microcalcifications have almost the same brightness level as the background tissue, which makes them difficult to detect. In view of the above, it is evident that methods for automatic detection of microcalcifications in mammograms are desirable in order to assist radiologists in the interpretation of mammograms and the diagnosis of breast cancer.

In this paper a new method to detect microcalcifications in mammograms is proposed. The method is based on a candidate selection procedure followed by a Support Vector Machine (SVM) classifier. During the candidate selection a 2-D linear prediction filtering is employed and a new measure based on the statistical distribution in a neighborhood is defined.

Method

In order to detect the microcalcifications we apply the following steps:

Candidate selection: We propose a method to select potential microcalcification points or candidate pixels for subsequent analysis and detection of microcalcifications. The method consists of two main steps:

1) 2D linear prediction error filtering [4,5], followed by thresholding. A pixel is selected as a pre-candidate for microcalcification if its prediction error is greater than an adaptively determined threshold. We use the multichannel version of the Burg algorithm to calculate this error. The multichannel version of the Burg algorithm calculates the optimal prediction coefficients, for a $p_1 \times p_2$ 2D predictor, by computing the prediction errors of order p_1. The prediction errors are represented as vectors of size $p_2 \times 1$ and are computed recursively, beginning with the 0-order prediction errors. The error values are initialized to the original image. The prediction errors of higher orders are calculated by repeating recursively the following three steps, with $i = 0,1,\cdots, p_1 - 2$:

1. Compute the covariance matrices for the forward and backward prediction errors as:

ISSN: 1727-1983

$$E_i^f = \sum_m e_i^f[m]\left(e_i^f[m]\right)^T$$
$$E_i^b = \sum_m e_i^b[m]\left(e_i^b[m]\right)^T \quad (1)$$
$$E_i^{bf} = \sum_m e_i^f[m]\left(e_i^b[m]\right)^T$$

where $e_i^f(m)$ and $e_i^b(m)$ are, respectively, the forward and backward prediction errors of order *i.* As both of the error vectors are of size $p_2 \times 1$, E_i^f, E_i^b and E_i^{bf} will be $p_2 \times p_2$ matrices. The summation, depending on *m*, is performed for all the prediction error vectors of size $p_2 \times 1$ that the subimage can be partitioned into.

2. Calculate the prediction coefficient matrix $A_{i+1}[i+1]$ by solving the following equation:

$$E_i^b A_{i+1}[i+1] + A_{i+1}[i+1]E_i^f = -2E_i^{bf} \quad (2)$$

3. Compute the backward and forward prediction error vectors of the higher prediction order as:

$$e_{i+1}^f[m] = e_i^f[m] + A_{i+1}[i+1]e_i^b[m-1]$$
$$e_{i+1}^b[m] = e_i^b[m-1] + A_{i+1}^T[i+1]e_i^f[m] \quad (3)$$

Once prediction errors are calculated for all the pixels in the image, they are thresholded to select pre-candidates pixels. The threshold is adaptively determined based upon the local average intensity of the subimage, local average value of the prediction error, and the global intensity (grey level) of the whole image.

This is based upon the observation that a microcalcification can be seen as a point of nonstationarity in an approximately homogeneous region or neighborhood in a mammogram. Such a pixel cannot be predicted well by the linear predictor, and hence leads to a high prediction error [6].

2) Calculation of a statistical parameter called tail ratio (*TR*), for the pre-candidates, followed by thresholding. Microcalcifications represent small points of high intensity. Therefore, if we analyze the probability density function (*pdf*) of the pixels belonging to a neighborhood surrounding a microcalcification, it will have the right tail longer than the left one. Based on this observation, we have developed a parameter, *TR*, that is a relative measure of the tail length of a *pdf*. There are some descriptors in the literature that measure the heaviness of the tail of a *pdf*. The kurtosis coefficient is often regarded as a measure of the heaviness of a distribution relative to the normal distribution. Its interpretation and use have been restricted to symmetric distributions, because of its intrinsic comparison with the symmetric normal distribution. Another disadvantage with kurtosis is that it is sensitive to outliers in the data, because it is based on moments of the data. For any distribution function *F* with finite moments, kurtosis is defined as:

$$k = \frac{E_F\left(X - E_F(X)\right)^4}{\left\{E_F\left(X - E_F(X)\right)^2\right\}^2} \quad (4)$$

where the numerator and denominator represent the second and fourth central moments of *F*, respectively and *X* are the data values. Some authors have presented other robust measures of kurtosis, but defined only for symmetric distributions, or merely measuring the peakedness instead of the tail weight [7,8].

Other works overcome the problems mentioned above by introducing several measures of tail weight for univariate continuous distributions that can be applied to symmetric as well as asymmetric distributions [9]. They define left and right tail measures as measures of skewness that are applied to the half-portion of the probability mass lying to the left or the right, respectively, of the median of *F*, denoted as $m_F = F^{-1}(0.5)$. Nevertheless, we have not found these measures capable of solving the problem of detecting microcalcifications, because they are an estimation of the heaviness of the tail but not of its length. Microcalcifications, as described above, are characterized by a long right tail in the local histogram. Therefore, in order to characterize the right tail, we have developed the tail ratio (*TR*), defined as:

$$TR = \frac{x_{\max} - F^{-1}(0.5)}{F^{-1}(0.5) - x_{\min}}, \quad (5)$$

where $x_{\max}$ and $x_{\min}$ represent the maximum and minimum intensity values of the *pdf* and F^{-1} is the inverse function of the probability distribution function. Because the size of a microcalcification is variable, the neighborhood around the pre-candidates used to calculate the local histogram must be adaptive. According to the size of a microcalcification, with the diameter varying from 0.1 to 1 mm, and according to the resolution of the database of images to be used, microcalcifications can occupy from 4 to 400 pixels each. Therefore, we initially calculate the histogram and the parameter *TR* for a 3×3 pixel square around each pre-candidate. If *TR* is over the applicable threshold, the pre-candidate is considered to be a candidate for the subsequent steps for the detection of microcalcifications. Otherwise, the square box is increased in size, and *TR* is recalculated. This procedure is repeated until one of the following two possible conditions is fulfilled: 1) the selection box reaches its maximal area (specified as 20×20 pixels in the present work), or 2) *TR* is higher than the applicable threshold. This procedure is summarized in Figure 1 After this step, the candidates are prepared for subsequent classification as a microcalcification or not.

ISSN: 1727-1983

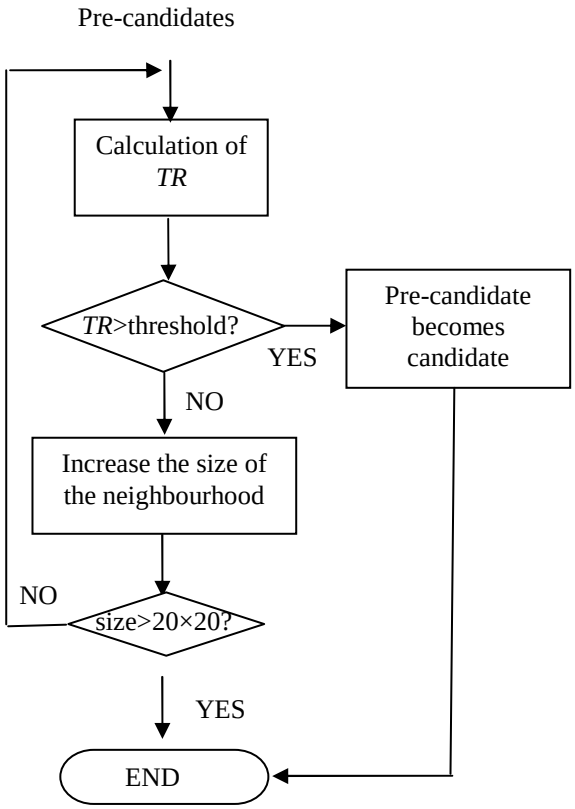

Figure 1: Scheme to select the candidates for microcalcifications.

Feature extraction: For each candidate for microcalcification, statistical texture features are extracted that, after a selection procedure, will be the inputs to a classifier. More specifically, the descriptors chosen for each candidate are:

1) Size of the square neighborhood (k) where TR exceeded the threshold.
2) TR value.
3) Inter-distance (ID): The parameter ID is based on the fact that pixels that have high intensity values (above the 98th percentile) will belong to a microcalcification, if present in the selected square neighborhood. In such a case, the pixels must be close to one another. Therefore, we define a new parameter, ID, calculated as:

$$ID = \frac{1}{N}\sum_{i=1}^{N}\sqrt{(x_i - x_c)^2 + (y_i - y_c)^2} \qquad (6)$$

where N is the number of pixels above the 98th percentile, (x_i, y_i) are the coordinates of the pixels selected, and (x_c, y_c) are the coordinates of the centroid of the selected pixels.
4) Average of the mean slopes (MS). In the four possible directions (North, South, East, and West), the mean descending slope from the pixel of maximum value in the neighborhood $k\times k$ is calculated, and MS is obtained as its average according to the equation

$$\begin{aligned} MS = \frac{1}{4}\cdot\frac{1}{(k/6)+1}\Big(&\sum_{n=n\max}^{n\max-k/6}\big[x(n-1,m)-x(n,m)\big]+\\ &+\sum_{n=n\max}^{n\max+k/6}\big[x(n+1,m)-x(n,m)\big]+\\ &+\sum_{m=m\max}^{m\max-k/6}\big[x(n,m-1)-x(n,m)\big]+\\ &+\sum_{m=m\max}^{m\max+k/6}\big[x(n,m+1)-x(n,m)\big]\Big) \end{aligned} \qquad (7)$$

where $n$max and $m$max are the coordinates of the pixel with the maximum value inside the neighborhood. The interval we have chosen to average the slope is k/6 because the estimated diameter of the microcalcification is k/3 in the $k\times k$ square.
5) Average of maximum slopes ($MaxS$). This feature represents the average of the maximum slopes in the North, South, East, and West directions of a candidate according to

$$\begin{aligned} MS = \frac{1}{4}\Big(&\max_{n\max\ge n\ge n\max-k/6}\big[x(n-1,m)-x(n,m)\big]+\\ &+\max_{n\max\le n\le n\max+k/6}\big[x(n+1,m)-x(n,m)\big]+\\ &+\max_{m\max\ge m\ge m\max-k/6}\big[x(n,m-1)-x(n,m)\big]+\\ &+\max_{m\max\le m\le m\max+k/6}\big[x(n,m+1)-x(n,m)\big]\Big) \end{aligned} \qquad (8)$$

6) Entropy (Ent) is defined as

$$Ent = -\sum_{j=0}^{N-1}P(j)\log_2(P(j)),$$

where N represents the number of grey values in the image and $P(j)$ is the probability of occurrence of grey value j.
7) Average height (AH) of the histogram inside the $k\times k$ neighborhood. This parameter is defined as $AH = \frac{\sum_{j=0}^{N-1}h(j)}{(\max(X)-\min(X))}$, where h represents the histogram of the data distribution X inside the $k\times k$ area.
8) Correlation with a Gaussian distribution (CG) with standard deviation equal to k/6. Although microcalcifications vary in form, it is considered a plausible assumption that they have a circularly symmetric Gaussian distribution [2, 10]. Therefore, if a microcalcification is present in the square region being analyzed, the correlation evaluated between the Gaussian and the image centered at the maximum within the square will be close to 1, if both signals have their energy normalized to 1.
9) Contrast parameter (C), calculated as $C = \frac{mean_k - m}{mean_k + m}$, where $mean_k$ is the average value of the pixels inside the $k\times k$ square and m represents

ISSN: 1727-1983

the mean value of the pixels belonging to the 2-pixel wide border of the square.

10) Dynamic range (*DR*), obtained as $DR = \max(X) - \min(X)$, where X represents the image values in the $k \times k$ square.

Feature selection

After analysis of the features described above, we found that it was necessary to apply a feature selection method to obtain the optimal set of features for the subsequent step of classification. The discriminant power of the 10 features was analyzed using the SFS method and the Sequential Backward Selection (SBS) method [11] via an SVM, which is described below.

SFS is a bottom-up search procedure where one feature at a time is added to the current feature set. At each stage, the feature to be included in the feature set is selected from the remaining available features that have not been added to the feature set yet, such that the new enlarged feature set yields a lower classification error as compared to adding any other single feature. The algorithm stops when adding a new feature leads to an increase in the classification error.

The SBS is the top-down counterpart of the SFS method. It starts from the complete set of features and, at each stage, the feature that shows the least discriminant power is discarded. The algorithm stops when removing another feature implies an increase in the classification error.

To analyze the two feature selection methods, we used five mammograms and selected 230 microcalcifications and 400 points that were not microcalcifications. Of the selected points, 184 microcalcifications and 320 non-microcalcifications were used as the training set for the classifier, and the remaining 46 microcalcifications and 80 non-microcalcifications as the test set. The selection performance was evaluated by five-fold cross validation (XVAL) [11], where the procedure is repeated five times, changing each time the training and the test sets and the average results are computed. In this manner, the disadvantage of the sensitivity of the SBS and SFS methods to the order of presentation of the training set is diminished [11].

In order to perform the SBS and SFS methods, a classifier is required. For this purpose, an SVM was used, as explained below.

The results of applying the SFS and SBS methods are summarized in Table 1. The average error was calculated by counting the misclassifications and dividing by the total number of microcalcifications. From Table 1, we see that the SFS method gives the best feature set [mean slope (*MS*), correlation with a Gaussian distribution (*CG*), contrast (*C*), dynamic range (*DR*), average height (*AH*), inter-distance (*ID*)], with an average error of 4.13%.

Table 1: Results of the SFS and SBS methods for feature selection.

Method	Feature set	Average error
SFS	*MS, CG, C, DR, AH, ID*	4.13%
SBS	*TR, AH, CG, C, DR*	4.92%

Detection of microcalcifications

After the features were selected, they were used to classify the candidates as microcalcifications or not. As mentioned before, the classifier chosen is an SVM. Support vector algorithms [12] constitute one of the important advances in computational learning in the 1990s. An SVM is the final step in a long research study known as statistical learning, carried out mainly by Vapnik [13]. Vector machine formulation is based on the principle of structural risk minimization (SRM), which has been shown to be better than the principle of empirical risk minimization; the latter method is used by many conventional neural networks. The principle of SRM consists of finding the subset of functions that minimizes the bound on the actual risk.

The advantages of SVM can be summarized as follows:

1) The training is a problem of convex quadratic programming. Computationally efficient algorithms are available for this purpose, and the finding of the global extremum is guaranteed.
2) The method does not face the problem of overfitting, as in the case of neural networks.
3) It allows to work with nonlinear relationships between the data (it generates nonlinear functions by means of kernels).
4) It generalizes well with a small number of training samples.

The kernel used is a Gaussian function with variance equal to 2.0.

Results

The detection algorithm was tested with 38 mammograms containing a total of 3,791 microcalcifications of different nature and diagnosis. The mammograms were obtained from Screen Test: The Alberta Program for the Early Detection of Breast Cancer [14]. The films were digitized with a Lumiscan 85 laser scanner (Lumisys, Sunnyvale, CA) with a spatial resolution of 50μm and 12 bits per pixel. Figure 2 shows a 258×422 pixel portion of a mammogram with microcalcifications. The backward and forward prediction error filtering was performed, obtaining the pre-candidates for microcalcifications. These points are centered at the maximal values in the surrounding area, so that they will be at the centers of the possible microcalcifications. In Figure 3 the pre-candidate points are shown as small black points.

The second part of the detection algorithm consists of calculating the *TR* parameter in order to select the final candidates for microcalcification from the set of pre-candidates. In Figure 3 we can see the result of this step of the algorithm, showing the candidates

ISSN: 1727-1983

surrounded by a black square. In Figure 4, the final result with the complete detection of the microcalcifications is shown.

The results obtained with the algorithms described were examined by an expert radiologist specialized in mammography (JELD), who determined the accuracy of the detection. The results are summarized in Table 2 and Table 3. It has to be noted that the numbers of true positives (TP) and false positives (FP) are calculated counting each individual microcalcification and not clusters. This fact should be considered when comparing the algorithm with other existing methods. From Table 3, we can observe that the method attains a sensitivity value of 0.93, a specificity value of 0.99 and a Positive-Predictive Value (PPV) of 0.89. The computational cost of the algorithm, when run on a Pentium 4 at 3.06 GHz and with 1GB DDR, was a processing time of 25s per mammogram, on the average.

Table 2: Performance analysis of the algorithm for detection of microcalcifications with 38 mammograms containing a total of 3,791 microcalcifications.

Total no. of pre-candidates	Total no. of candidates	TP	TN	FP	FN
189,251	43,753	3,536	39,468	494	255

Table 3: Parameters for the evaluation of the algorithm for detection of microcalcifications with 38 mammograms containing a total of 3,791 microcalcifications.

Sensitivity	PPV	Specificity
0.93	0.89	0.99

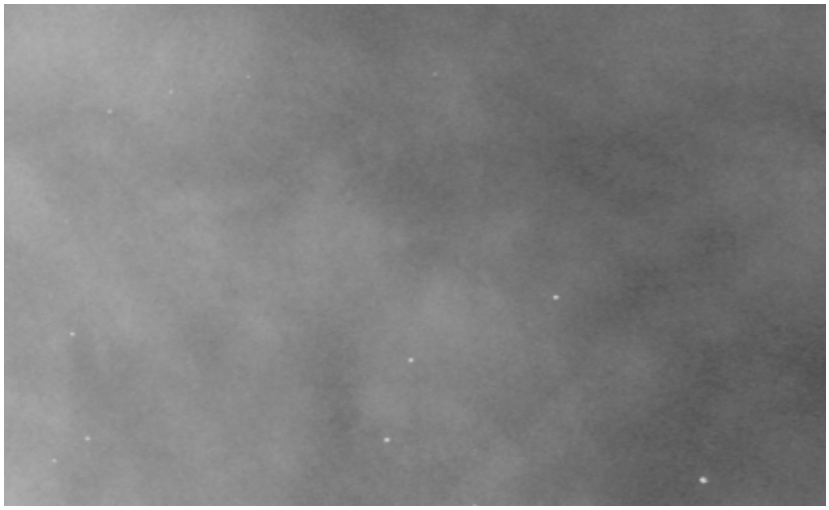

Figure 2: A 258×422 pixel portion of a mammogram with microcalcifications.

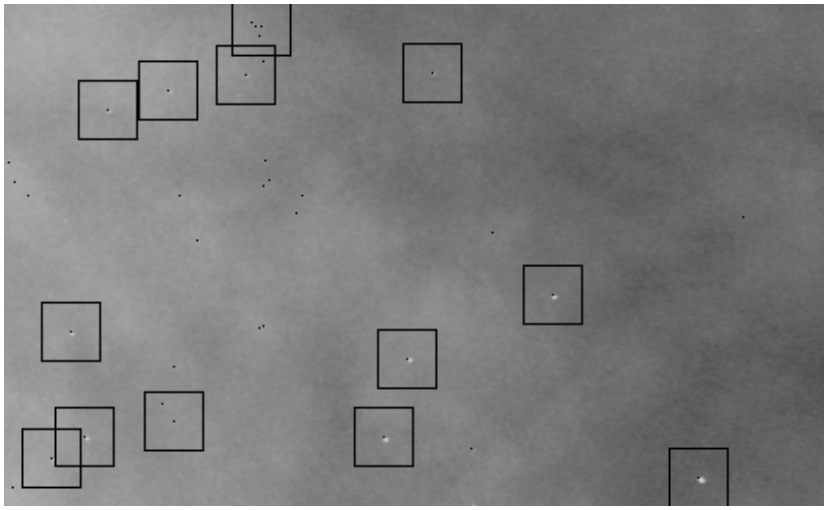

Figure 3: Pre-candidates for the detection of microcalcifications shown as small black points and candidates for microcalcifications shown surrounded by a black square.

ISSN: 1727-1983

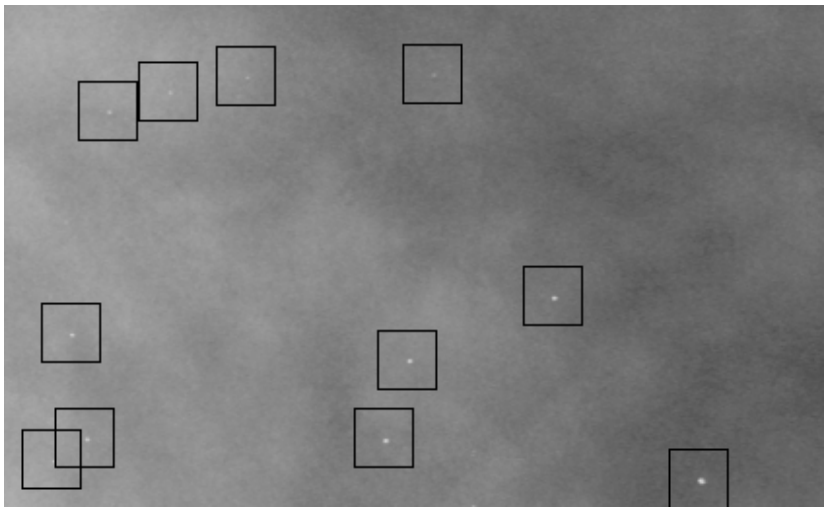

Figure 4: Final results of detected microcalcifications.

Conclusions

In this paper a CAD tool to help the radiologist to diagnose microcalcifications has been presented. It automatically detects microcalcifications in mammograms. The method has been tested with 38 mammograms from the Calgary database. The results obtained with the method are very promising for the sensitivity is 0.93 for a PPV of 0.89.

References

[1] SHEN L., RANGAYYAN R.M. , AND DESAUTELS J.E.L. (1993): 'Detection and Classification of Mammographic Calcifications', *International Journal of Pattern Recognition and Artificial Intelligence*, **7** (6), pp. 1403-1416.

[2] STRICKLAND R.N. AND HAHN H.I. (1996): 'Wavelet Transforms for Detecting Microcalcifications in Mammograms', *IEEE Trans. on M*edical Imaging, 15, pp. 218-229.

[3] CHENG H.D., CAI X., CHEN X., HU L. AND LOU X. (2003): 'Computer-aided detection and classification of microcalcifications in mammograms: a survey', *Pattern Recognition*, **36**, pp. 2967-2991.

[4] KUDUVALLI G.R. AND RANGAYYAN R.M. (1993): 'An algorithm for direct computation of 2-d linear prediction coefficients', *IEEE Trans. on Signal Processing*, **41**, pp. 996-999.

[5] KUDUVALLI G.R. AND RANGAYYAN R.M. (1992): 'Performance analysis of reversible image compression techniques for high-resolution digital teleradiology', *IEEE Trans. on Medical Imaging*, **11**, pp. 430-445.

[6] SERRANO C., DÍAZ J., ACHA B. AND. RANGAYYAN R.M (2001): 'Use of linear prediction error to detect microcalcifications in mammograms', *Proc. of II Latinoamerican Conf. on Biomedical Eng.*, La Habana, Cuba, 2001.

[7] GROENEVELD R.A. (1984): 'A class of quantile measures for kurtosis', *The Statistician*, **33**, pp. 391-399.

[8] SCHMID F. AND TREDE M. (2003): 'Simple tests for peakedness, fat tails and leptokurtosis based on quantiles', *Comput. Statist. Data Anal.*, **43**, pp. 1-12.

[9] BRYS G., HUBERT M. AND STRUYF A. (2005): 'Robust measures of tail weight', *Computational Statistics & Data Analysis*, article in press (available online at www.sciencedirect.com).

[10] BOCCHI L., COPPINI G., NORI J. AND VALLI G. (2004): 'Detection of single and clustered microcalcifications in mammograms using fractals models and neural networks' *Med. Eng. & Physics*, **26**, pp. 303-312.

[11] FUKUNAGA K. (1990): 'Introduction to Statistical Pattern Recognition', 2nd edition, (Morgan Kaufmann, Academic Press).

[12] BURGES C.J.C. (1998): 'A tutorial on support vector machines for pattern recognition', *Data Mining and Knowledge Discovery*, **2**, pp. 121-167.

[13] VAPNIK V. (1995): 'The Nature of Statistical Learning Theory', (Springer-Verlag, New York).

[14] ALBERTA CANCER BOARD (2004): 'Screen Test: Alberta Program for the Early Detection of Breast Cancer', 2001/03 Biennial Report, Edmonton, Alberta, Canada.

ISSN: 1727-1983